1. Classification *INPE-COM.4-RPE*
C.D.U.: 539.2

2. Period

4. Distribution Criterion
internal [ ]
external [X]

3. Key Words (selected by the author)
BAND THEORY
SEMICONDUCTOR

5. Report Nº
INPE-1799-RPE/169

6. Date
June, 1980

7. Revised by
Ronald Ranvaud

8. Title and Sub-title
"SELF-CONSISTENT APW-$\vec{k}.\vec{p}$ METHOD II APPLICATION TO NaCl"

9. Authorized by
Nelson de Jesus Parada
Director

10. Sector *DEE* Code

11. Nº of Copies *10*

12. Authorship
I.C.da Cunha Lima
A. Ferreira da Silva
N.J.Parada

13. Signature of the responsible

14. Nº of Pages *28*

15. Price

16. Summary/Notes

The self-consistent APW.-$\vec{k}.\vec{p}$ method is utilized to obtain the band structure of NaCl in the "muffin-tin" approximation. We have investigated the convergence of many intermediate results, e.g, crystalline potential, matrix elements of the momentum operator and energy eigenvalues at the Γ point. The summation on the reciprocal space, included in the definition of the matrix D of the theory, is performed by direct sum and also by special points technique. For the convergence criteria used, the results converged after five iterations.

17. Remarks *This paper will be submitted to International Journal of Quantum Chemistry.*

SELF - CONSISTENT APW - $\vec{k}.\vec{p}$ METHOD

II - APPLICATION TO NaCl

I.C. da Cunha Lima, A. Ferreira da Silva and N.J. Parada

Instituto de Pesquisas Espaciais, INPE, Conselho Nacional de Desenvolvimento Científico e Tecnológico, CNPq, 12200 São José dos Campos, São Paulo, Brazil

ABSTRACT

The self-consistent APW- $\vec{k}.\vec{p}$ method is utilized to obtain the band structure of NaCl in the "muffin-tin" approximation. We have investigated the convergence of many intermediate results, e.g, crystalline potential, matrix elements of the momentum operator and energy eigenvalues at the Γ point. The summation in reciprocal space, included in the definition of the matrix D of the theory, is performed by direct sum and also by a special points technique. For the convergence criteria used, the results converged after five iterations.

1. INTRODUCTION

In a preliminary article [1] the authors have presented the formalism of a self-consistent APW-$\vec{k}.\vec{p}$ method for electronic energy bands calculation. In this introduction, we summarize the main features of this formalism.

Let assume that the results of an APW calculation are known at a high symmetry point $\vec{k}_0$. The Bloch function at a general point $\vec{k}$ may be determined by a Kohn-Luttinger expansion [2] .This enables us to obtain a secular equation to calculate the energy eigenvalues and the expansion coefficients. This scheme is called $\vec{k}.\vec{p}$ [3] .

The self-consistent density of charges inside each sphere p of the "muffin-tin" model is given by

$$\sigma_p(r) = 2er^2 \sum_{\substack{m,m' \\ m\geq m'}} n_\alpha \left\{ 2\ \mathrm{Re}\ \left[D^\alpha_{mm'} I^\alpha_{mm'}(r) \right] - \delta_{mm'} \mathrm{Re}\left[D^\alpha_{mm'} I^\alpha_{mm'}(r) \right] \right\} \qquad (1)$$

with Re for real part, and

$$D^\alpha_{mm'} = \frac{g}{n_\alpha} \cdot \frac{1}{G} \sum_{n,i} \sum_{\vec{k}}^{ZB/g} \sum_{\ell} \frac{A^{m,\ell}_{n,i}(\vec{k})^* A^{m,\ell}_{n,i}(\vec{k})}{W(\vec{k})} \qquad (1a)$$

$$I^\alpha_{mm'}(r) = \sum_{\vec{K}_s,\vec{K}_T} \left\{ \sum_{\ell,t} C^{\Gamma^\alpha}_{m\ell}(\vec{K}_s)^* C^{\Gamma^\alpha}_{m't}(\vec{K}_T) \sum_{\lambda} \bar{u}_{p,\lambda,m}(r) \bar{u}_{p,\lambda,m'}(r)\ B^\alpha_p \right\} \qquad (1b)$$

and

$$B^\alpha_p = \frac{g}{n_\alpha} 4\pi(2\lambda+1) \sum_{\vec{R}} \Gamma^*_{\ell,t}(R) \exp\left[i(R\vec{K}_T - \vec{K}_s)\cdot \vec{r}_p \right] j_\lambda(K_s R_p) j_\lambda(K_T R_p) P_\lambda(\cos\gamma) \qquad (1c)$$

In (1a) g is the order of the group of the wave vector $\vec{k}_0$, n_α is the dimension of the representation Γ_α, and G is the number of vectors considered in the summation on the reciprocal space. As we have

mentioned before, the coefficients A are determined by diagonalization of the secular matrix of the $\vec{k}.\vec{p}$ expansion, Eq. (6) in Ref. 1. $W(\vec{k})$ are weights assigned to each vector in order to consider repetitions when the g operations of symmetry are applied to it. Summation involves only occupied states. In Eq. (1b) $\vec{k}$ represents the vectors of the reciprocal lattice and C the coefficients of expansion of the Bloch states at $\vec{k}_0$ in Symmetrized Augmented Plane Waves. The charge density is assumed to be constant outside the spheres and it has a value $\bar{\rho}$ such that the unitary cell is electrically neutral. The crystalline potential is assumed spherically symmetric inside spheres and zero outside. The former is a sum of a Coulomb and an exchange term,

$$V_p^{Coul}(r) = -\frac{2Z_p}{r} + \frac{2}{r}\int_0^r \sigma_p(t)\,dt + 2\int_r^{R_p} \frac{\sigma_p(t)}{t}\,dt + C_p \;;(r<R_p) \quad (2)$$

$$V_{exch} = -6\alpha\left[3\sigma_p(r)/32\pi^2r^2\right]^{1/3} + 6\alpha(3\bar{\rho}/8\pi)^{1/3} \;;\; (r<R_p) \quad (3)$$

where α is a parameter that takes the value 1 in the Slater's[4] approximation, 2/3 in the Kohn and Sham[5] method or may be adjusted to fit the experimental results. Many other approximations include many body effects in the exchange term in order to get a more accurate potential. We restricted ourselves to the use of α=1.

Once we have calculated the average value of the potential in the plane wave region, V^{out}, and its average value on the surface of the spheres, $V(R_p)$, we obtain C_p, as indicated in Ref. 1:

$$\frac{-2Z_p}{R_p} + \frac{2}{R_p}\int_0^{R_p} \sigma_p(r)\,dr + C_p = V(R_p) - V^{out} \quad (4)$$

We used this method to calculate the band structure for NaCl. Section 2 deals with the first iteration. This part was done

preliminarily by Sans [6] and here we will present some of the results.

Section 3 concerns the iterative process, where we present the results obtained for the matrix elements of the momentum operator, matrix D, energy levels at the Γ point and the band structure. Comparison is made with Chadi and Cohen [7] special points.

Finally, in Section 4, we point out some possible improvements of the method and discuss some of its main characteristics and advantages.

2. INITIAL RESULTS AND DETAILS OF THE CALCULATION

The first iteration was performed starting with a crystalline potential obtained by the Superimposed-Free-Ion [8] (SFI) model using the Herman and Skilmman [9] ionic potentials. Fig. 1a and 1b show the radial functions for the ions Cl^- and Na^+. We calculated in the "muffin-tin" approximation the potential, the radii of the spheres and the average value of the crystalline potential outside the spheres. The values obtained for the radii, R_{Cl} = 2.86 a.u. and R_{Na} = 2.46 a.u. coincide with those of Clark and Kliewer [10] .

The APW calculation at the Γ point was performed with ℓ_{max}=13 in the expansion of spherical harmonics and with Wood's quadrivectors [11] indicated in Table I. Table II presents some parameters used.

Since the NaCl structure does contain an inversion center, the matrix elements of the momentum operator are real. Their values, calculated in the initial iteration, are shown in the first column of Table III. Once we have obtained the results at the Γ point, i.e., energy levels, coefficients of the APW expansion, and matrix elements of the momentum operators, we begin the self-consistent process. First,

we calculate the radial function $\bar{u}_{n\ell}(r)$, defined for each sphere as

$$\bar{u}_{n,\ell}(r) = u_{n,\ell}(r)/u_{n,\ell}(R_p)$$

in the 200 point mesh of the APW. We obtain, separately, the values of B_p^α according to Eq. (1c). This part is done only once in the whole process since B_p^α depends only on the symmetry of the crystal and on the sphere radii.

Once we have obtained the coefficients of the $\vec{k}.\vec{p}$ expansion, we perform the summation in the reciprocal space volume corresponding to 1/48 of the first Brillouin zone, taking into account only the occupied states. This fraction of the B.Z. is limited by the Γ-L-K-W-P-X points, as shown in Fig. 2. It corresponds to a set of vectors $\vec{k}$ such that

$$k_x > k_y > k_z$$
$$k_x < 2\pi/a$$
$$k_x + k_y + k_z < 3\pi/a$$

If we use N vectors $\vec{k}_i$ in this region, it corresponds to performing the summation taking into account N_{total} vectors in the whole B.Z., given by

$$N_{total} = \sum_{i=1}^{N} \frac{48}{W(\vec{k}_i)}$$

At this point, we used two different approaches. The first one considering N equal to 28 (the vectors are shown in Table IV). The second one considering N equal to 152, N_{total} corresponding to 500 and 4000 vectors respectively. The matrix D was calculated in both approaches for each iteration.

With these partial results, we obtained the charge density inside

each sphere according to Eq. (1). Later, we calculated the crystalline potential with Eq. (2) and (3), and constant C_p according to the Appendix A of Ref. 1.

In order to assure uniform convergence, we used as the starting potential for the second iteration that obtained as the arithmetic average between the starting and the resulting potentials of the first iteration. But for the following iterations, we used two criteria, the first one being a continuation of this procedure and the second one by alternating the Pratt [8] criteria with the arithmetic average.

3. RESULTS OF THE SELF-CONSISTENCY

We have obtained good convergence after only 5 iterations. The energy levels at the Γ point are shown in Table V. We can observe that the Pratt criterion gave a faster convergence. This was achieved not only in the energy levels but also in the other results. The self-consistency showed a trend to decrease the energy gap, due to a bad choice of the initial value of the potential outside spheres. At the second iteration an inversion appeared between the levels $^1\Gamma_2$ and $^2\Gamma_{15}$ and remained in the following iterations.

Valence charges inside the spheres decreased through the process, increasing the plane wave component for each level. The variations, however, were very small. The levels $^1\Gamma_1$ and $^1\Gamma_{15}$, at the end of the calculation, were composed respectively of 93% of the $3s^2$ state and 94.8% of the $3p^6$ of the Cl^-, as shown in Table VI.

The matrix elements of the momentum operator for the first and the last two iterations are shown in Table III.

When compared with the results obtained by Sans [6] , we notice

that the biggest discrepancies occur with the values of $M_1^2;{}^2_{1S}$ and $M_1^3;{}^1_{1S}$. But these discrepancies are not important since the values are very small and the levels involved are very distant in energy.

Tables VII show the important elements of matrix D in the first and last iteration. We can observe that the differences between the results with 500 and 4000 vectors are not significant. Through the five iterations, the value changed less than 1%. In the last iteration, we made a test using the Chadi and Cohen [7] special points, i.e., we returned to the $\vec{k}.\vec{p}$. expansion and performed the calculation of the coefficients with 1,2 and 10 special points. They are shown in Table VIII with their coordinates and respective weights. In this case, the principal part of the matrix D appears in Table IX. The results tend to converge to the same values in both cases, i.e., the direct sum and the use of special points.

We see that the Chadi and Cohen [7] theory gave good results but we have to keep in mind that the valence energy levels are well localized in NaCl.

Fig. 3 shows the self-consistent crystalline potential in atomic units. Fig. 4 shows the band structure in the symmetry directions, i.e., axes Λ, Δ and Σ.

4. CONCLUSION

The article of Roessler and Walker [12] on optical-reflectance spectra of NaCl suggests a gap between Γ_{1S} and Γ_1 of 8.97 eV. Gout and Pradal [13] measuring the energy losses of electron in alkali-halides suggest E_g = 8.7 eV for NaCl. Measurements of photoemission have been performed by Haensel et al [14] who obtained a gap of

8.5 eV. More recently Himpsel and Steinmann [15] obtained E_g = 9.0 eV from measurements of angle-resolved photoemission. On the other hand many theoretical calculations have been performed in NaCl. Melvin and Smith [16] obtained E_g = 5.0 eV using APW method. Kunz [17] using the OPW method with a superimposed free ion potential and Slater's exchange obtained E_g = 7.4 eV.Fong and Cohen [18] adjusted the gap $\Gamma_{1s} \rightarrow \Gamma_1$ to 8.97 eV and calculated the electronic band structure by the empirical pseudopotential method. Perrot [19] used the APWHF(Hartree--Fock APW) method and obtained E_g = 8.4 eV. Lipari and Kunz [20] calculated the energy bands and optical properties of NaCl using a mixed basis method. The calculations were performed only at the points Γ,X and L and the medium point of Δ. They adjusted the valence bands with tight binding expressions and the conduction bands with a pseudo--Hamiltonian. The gap obtained was 10.0 eV. In Table X we compare our results with some of the measurements and calculations mentioned above. It is worthwhile to point out that a better choice of the exchange potential and corrections to the "muffin-tin" should be the next step to this self-consistent APW-$\vec{k}.\vec{p}$ calculation in order to better fit the experimental results of the gap energy and valence bandwidth and at the same time, to better understand the importance of the different aproximations normally imposed. In this direction, Kunz et al[21] have already carried out the calculations using different kinds of crystalline potential and comparing their results with many of the works mentioned in this article. Recently Closs[22] introduced "non muffin-tin" corrections into the APW-$\vec{k}.\vec{p}$ method in a self-consistent way. He concluded that the calculations become overwhelming, at least in the case of GaAs, with no inversion center.

We conclude by presenting some characteristics of this self-consistent method.

1. For structures, like NaCl, the method proved to converge very quickly, not only for the energy levels at the Γ point, but also for the matrix elements of momentum, matrix D and crystalline potentials.
2. The matrix D changed very weakly throughout the iterative process and does not depend too much on the number of points in the B.Z. This method can be even faster if we calculate the matrix D with the 10 points of Chadi and Cohen [7] only in the first iteration.
3. The use of APW calculation only once per iteration and at the Γ point, makes this self-consistency easy to manipulate and extremely time-saving.
4. The use of the Ewald-Slater method [23] makes this method applicable to any structure.

Guimarães [24] has used our results to calculate the effective mass for the conduction band. He obtained the value $m^*/m_0=0.5012$. Page and Hygh [25] obtained the value 0.573, using a non-self-consistent APW calculation.

FIGURES CAPTIONS

Fig. 1a Square modulus of radial functions of the ion Cl^- in fundamental state.

Fig. 1b Square modulus of radial functions of the ion Na^+ the fundamental state.

Fig. 2 First Brillouin zone for fcc structure.

Fig. 3 Self-consistent crystalline potential in the direction (0,0,1) obtained by the Pratt criteria for NaCl.

Fig. 4a Band structure of NaCl in the Δ axis.

Fig. 4b Band structure of NaCl in the Λ axis.

Fig. 4c Band structure of NaCl in the Σ_1 axis.

REFERENCES

[1] I.C. da Cunha Lima, A. Ferreira da Silva and N.J. Parada - Part I of this series

[2] J.M. Luttinger and W. Kohn, Phys. Rev. 97 869 (1955).

[3] N.J.Parada, Phys. Rev. B3, 2042 (1971).

[4] J.C. Slater, Phys. Rev. 81, 385 (1951).

[5] W. Kohn and L.J. Sham, Phys. Rev. 140, 1133 (1965).

[6] T.T. Sans, M. Sc. Thesis, Instituto de Física "Gleb Wataghin", UNICAMP, Campinas, Brazil (1973) (unpublished).

[7] D.J. Chadi and M.L. Cohen, Phys. Rev. B8, 5747 (1973).

[8] For a very complete review on APW method see L.F. Matheiss, J.H. Wood and A.C. Switendick in "Methods in Computational Physics", vol. 8, chapt. 4, Academic Press (1968).

[9] F. Herman and S. Skilman, "Atomic Structure Calculations", Prentice Hall (1963).

[10] T.D. Clark and K.L.Kliewer, Phys. Letters, 27A 167 (1968).

[11] J.H. Wood - APW Manual, M.I.T. (unpublished).

[12] D.M. Roessler and W.C. Walker, Phys. Rev. 166, 599 (1968).

[13] G. Gout and F. Pradal, J. Phys. Chem. Solids, 29, 581 (1968).

[14] R. Haensel, G. Keitel, G. Peters, P. Schreiber, B. Sonntag and C. Kunz, Phys. Rev. Letters, 23, 530 (1969).

[15] F.J. Himpsel and W. Steinmann, Phys. Rev. B17, 2537 (1978).

[16] J.S. Melvin and T. Smith, Phys. Status Solidi B49, 173 (1972).

[17] A. Barry Kunz, Phys. Rev. 175, 1147 (1968).

[18] C.Y. Fong and Marvin L. Cohen, Phys. Rev. 185, 1168 (1969).

[19] F. Perrot, Phys. Status Solidi B52, 163 (1972).

[20] Nuzio O. Lipari and A. Barry Kunz, Phys. Rev. B3, 491 (1971).

[21] A.B. Kunz, W.B. Fowler and P.M. Schneider, Phys. Letters 28A,553 (1969).

[22] H. Closs, Ph.D. thesis, Instituto de Física "Gleb Wataghin", UNICAMP, Campinas, Brazil (1979) (unpublished).

[23] J.C. Slater, Quantum Theory of Molecules and Solids, Vol. 1, Appendix 12, McGraw Hill (1963).

[24] P.S. Guimarães (private communication).

[25] L.J. Page and F.H. Hygh, Phys. Rev. B1, 3472 (1970).

TABLE I - Quadrivectors used in the expansion of the Bloch functions at the Γ point (in units of $2\pi/a$). According to Wood, the fourth indices indicate the sign of representation and partner.

Γ_1	Γ_{25*}	Γ_{2*}	Γ_{15}	Γ_{12}
0 0 0 1	2 2 2 -1	2 2 2 -1	2 2 2 1	0 4 0 1
2 2 2 1	4 0 4 -2	2 6 2 -1	0 4 0 2	4 0 4 1
0 4 0 1	2 6 2 -1	4 4 4 -1	4 0 4 1	2 6 2 1
4 0 4 1	2 6 2 -2	6 2 6 -1	2 6 2 1	0 8 0 1
2 6 2 1	4 4 4 -1	4 8 4 -1	2 6 2 2	6 2 6 1
4 4 4 1	6 2 6 -1	6 6 6 -1	4 4 4 1	0 4 8 1
0 8 0 1	6 2 6 -2	2 10 2 -1	0 8 0 2	0 4 8 2
6 2 6 1	0 4 8 -1	2 6 10 -1	6 2 6 1	4 8 4 1
0 4 8 1	4 8 4 -1	8 4 8 -1	6 2 6 2	2 10 2 1
4 8 4 1	4 8 4 -2	6 10 6 -1	0 4 8 2	8 0 8 1
6 6 6 1	6 6 6 -1	4 12 4 -1	0 4 8 3	2 6 10 1
2 10 2 1	2 10 2 -1		4 8 4 1	2 6 10 2
8 0 8 1	2 10 2 -2		4 8 4 2	0 12 0 1
2 6 10 1	8 0 8 -2		6 6 6 1	8 4 8 1
0 12 0 1	2 6 10 -1		2 10 2 1	0 4 12 1

TABLE II - Some parameters utilized in the APW calculation at the Γ point.

Lattice parameter	10.6577	au
Na^+ - radius of the APW sphere	2.46	au
Cl - radius of the APW sphere	2.96	au
Madelung energy - V_m	0.656	Ry
Mean value of the potential outside spheres	-0.145	Ry
Potential on the spheres surfaces	-0.777	Ry

TABLE III - Matrix elements (absolute value) of the momemtun operator obtained in the first and last two iterations in atomic units. A represents results with the arithmetic average and B those with Pratt's criteria.

ITERATION	1st	4th		5th	
		A	B	A	B
$M^{1}_{1;1}$	0.767332	0.76085	0.76090	0.76019	0.76037
$M^{1}_{1;1s}$	0.097747	0.09253	0.09561	0.09312	0.09462
$M^{2}_{1;1s}$	0.719985	0.71238	0.71343	0.71255	0.71192
$M^{2}_{1;1s}$	0.039463	0.03938	0.06455	0.05186	0.06528
$M^{3}_{1;1s}$	0.134412	0.05902	0.03518	0.04718	0.03437
$M^{3}_{1;1s}$	1.152127	1.17804	1.18037	1.17890	1.17930
$M^{1}_{12;1s}$	0.971589	0.96078	0.96481	0.96091	0.96265
$M^{1}_{12;1s}$	1.074235	1.10948	1.12233	1.11490	1.12050
$M^{1}_{2s;2}$	1.107032	1.12881	1.12738	1.12960	1.12890
$M^{1}_{2s;1s}$	0.977250	0.95030	0.95092	0.94811	0.94756
$M^{1}_{2s;1s}$	0.535707	0.59054	0.60007	0.59592	0.60196

TABLE IV - The mesh of 28 points in the fraction 1/48 of the Brillouin zone (in units of π/a)and their weights. They correspond to 500 points in the whole zone.

VECTOR	W(r)	VECTOR	W(r)	VECTOR	W(r)	VECTOR	W(r)
(0;0;0)	48	(0.4;0;0)	8	(0.4;0.4;0)	4	(0.4;0.4;0.4)	6
(0.8;0;0)	8	(0.8;0.4;0)	2	(0.8;0.8;0.4)	2	(0.8;0.8;0)	4
(0.8;0.8;0.4)	2	(0.8;0.8;0.8)	6	(1.2;0;0)	8	(1.2;0.4;0)	2
(1.2;0.4;0.4)	2	(1.2;0.8;0)	2	(1.2;0.8;0.4)	1	(1.2;0.8;0.8)	2
(1.2;1.2;0)	4	(1.2;1.2;0.4)	2	(1.6;0;0)	8	(1.6;0.4;0)	2
(2.0;0;0)	16	(2.0;0.4;0)	4	(2.0;0.4;0.4)	4	(2.0;0.8;0)	4
(1.6;0.4;0.4)	2	(1.6;0.8;0)	2	(1.6;0.8;0.4)	1	(1.6;1.2;0)	2

TABLE V - Energy levels in Rydbergs obtained at the Γ point

ITERATION	1st	2nd	3rd		4th		5th	
ENERGY LEVEL	SFI	Average	Average	Pratt	Average	Pratt	Average	Pratt
$^1\Gamma_1$	-1.4917	-1.3524	-1.3842	-1.3785	-1.2253	-1.2004	-1.2006	-1.1852
$^1\Gamma_{1s}$	-0.5618	-0.4161	-0.4344	-0.4243	-0.2853	-0.2601	-0.2599	-0.2436
$^2\Gamma_1$	0.0776	0.1683	0.1796	0.2348	0.2287	0.2594	0.2459	0.2632
$^1\Gamma_{2s}$	0.4686	0.5886	0.6095	0.6410	0.6792	0.7031	0.6980	0.7135
$^1\Gamma_{12}$	0.5447	0.6967	0.7180	0.7601	0.8137	0.8461	0.8390	0.8598
$^1\Gamma_2$	0.9196	0.9546	0.9657	0.9799	0.9791	0.9868	0.9843	0.9893
$^1\Gamma_{1s}$	0.8993	1.0217	1.0529	1.1550	1.1055	1.1569	1.1331	1.1623
$^3\Gamma_1$	1.4000	1.4973	1.5318	1.6429	1.5726	1.6268	1.5983	1.6277

TABLE VI - Distribution of states at the Γ point in plane wave and spherical harmonics for the last iteration using the Pratt's criteria.

REPRESENTATION	ENERGY	PLANE WAVE	ℓ = 0		ℓ = 1		ℓ = 2		ℓ = 3	
			Cl	Na	Cl	Na	Cl	Na	Cl	Na
$^{1}\Gamma_{1}$	-1.1852	3.96	95.27	0.74	0.00	0.00	0.00	0.00	0.00	0.00
$^{2}\Gamma_{1}$	0.2632	57.49	20.36	22.11	0.00	0.00	0.00	0.00	0.00	0.00
$^{3}\Gamma_{1}$	1.6278	44.31	0.44	49.26	0.00	0.00	0.00	0.00	0.00	0.00
$^{1}\Gamma_{12}$	0.8593	23.85	0.00	0.00	0.00	0.00	64.08	11.94	0.00	0.00
$^{1}\Gamma_{15}$	-0.2436	4.18	0.00	0.00	94.33	0.64	0.00	0.00	0.00	0.35
$^{2}\Gamma_{15}$	1.1623	39.73	0.00	0.00	3.49	45.94	0.00	0.00	10.66	0.07
$^{1}\Gamma_{2}$	0.9893	85.01	0.00	0.00	0.00	0.00	0.00	0.00	11.14	3.94
$^{1}\Gamma_{25}$	0.7135	43.47	0.00	0.00	0.00	0.00	48.35	7.82	0.00	0.00

TABLE VII a - The important part of matrix D calculated in the first iteration with 28 and 152 vectors in 1/48 of the BZ.

		$^1\Gamma_1$	$^1\Gamma_{1s}$	$^2\Gamma_1$	$^1\Gamma_{2s}^*$
$^1\Gamma_1$	28	0.9944	0.0000	-0.0354	0.0000
	152	0.9944	0.0000	-0.0354	0.0000
$^1\Gamma_{1s}$	28	0.0000	0.8073	0.0000	0.0000
	152	0.0000	0.8073	0.0000	0.0000
$^2\Gamma_1$	28	-0.0354	0.0000	0.0890	0.0000
	152	-0.0354	0.0000	0.0890	0.0000
$^1\Gamma_{2s}^*$	28	0.0000	0.0000	0.0000	0.0950
	152	0.0000	0.0000	0.0000	0.0950

TABLE VII b - The important part of matrix D calculated in the last iteration with the media criteria.

		$^1\Gamma_1$	$^1\Gamma_{15}$	$^2\Gamma_1$	$^1\Gamma_{25}*$
$^1\Gamma_1$	28	0.9933	0.0000	-0.0599	0.0000
	152	0.9934	0.0000	-0.0594	0.0000
$^1\Gamma_{15}$	28	0.0000	0.9246	0.0000	0.0000
	152	0.0000	0.9245	0.0000	0.0000
$^2\Gamma_1$	28	-0.0599	0.0000	0.1285	0.0000
	152	-0.0594	0.0000	0.1279	0.0000
$^1\Gamma_{25}*$	28	0.0000	0.0000	0.0000	0.0783
	152	0.0000	0.0000	0.0000	0.0791

TABLE VII c - The important part of matrix D calculated at the last iteration with Pratt's criteria with 28 and 152 vectors in 1/48 of the BZ.

		$^1\Gamma_1$	$^1\Gamma_{15}$	$^2\Gamma_1$	$^1\Gamma_{25}*$
$^1\Gamma_1$	28	0.9868	0.0000	- 0.0531	0.0000
	152	0.9879	0.0000	- 0.0539	0.0000
$^1\Gamma_{15}$	28	0.0000	0.8121	0.0000	0.0000
	152	0.0000	0.8147	0.0000	0.0000
$^2\Gamma_1$	28	- 0.0531	0.0000	0.1158	0.0000
	152	-0.0539	0.0000	0.1163	0.0000
$^1\Gamma_{25}*$	28	0.0000	0.0000	0.0000	0.0832
	152	0.0000	0.0000	0.0000	0.0839

TABLE VIII - Coordinates of the special points of Chadi and Cohen in the fraction of 1/48 of the B.Z. (units of $2\pi/a$). The weights are shown inside the brakets.

N = 1
1/2, 1/2,0 [1]
N = 2
3/4, 1/4, 1/4 [3/4] ; 1/4, 1/4, 1/4 [1/4]
N = 10
7/8, 3/8, 1/8 [3/16] ;7/8, 1/8, 1/8 [3/32]
5/8, 5/8, 1/8 [3/32] ;5/8, 3/8, 3/8 [3/32]
5/8, 3/8, 1/8 [3/16] ;5/8, 1/8, 1/8 [3/32]
3/8, 3/8, 3/8 [1/32] ;3/8, 3/8, 1/8 [3/32]
3/8, 1/8, 1/8 [3/32] ;1/8, 1/8, 1/8 [1/32]

TABLE IX - The matrix elements of D calculated with the Chadi and Cohen special points (1,2 and 10) for the last iteration.

		$^1\Gamma_1$	$^1\Gamma_{1s}$	$^2\Gamma_1$	$^1\Gamma_{2s}$*
$^1\Gamma_1$	1	0.9933	0.0000	-0.0599	0.0000
	2	0.9903	0.0000	-0.0550	0.0000
	10	0.9901	0.0000	-0.0561	0.0000
$^1\Gamma_{1s}$	1	0.0000	0.8247	0.0000	0.0000
	2	0.0000	0.8214	0.0000	0.0000
	10	0.0000	0.8172	0.0000	0.0000
$^2\Gamma_1$	1	-0.0599	0.0000	0.1286	0.0000
	2	-0.0550	0.0000	0.1134	0.0000
	10	-0.0561	0.0000	0.1201	0.0000
$^1\Gamma_{2s}$*	1	0.0000	0.0000	0.0000	0.0784
	2	0.0000	0.0000	0.0000	0.0826
	10	0.0000	0.0000	0.0000	0.0840

TABLE X - Differences in energy for the important band transitions at the points Γ, L and X. Energy in eV.

Band Transition	Roessler et al [12]	Gout et al [13]	Himpsel & Steinmann [15]	Kunz [17]	Lipari & Kunz [20]	Page & Hygh [25]	Perrot [19]	Fong & Cohen [18]	S.C.APW-$\vec{k}.\vec{p}$
$\Gamma_{15} \rightarrow \Gamma_1$	8.97	8.7	9.0	7.4	10.0	8.78	8.4	8.97	6.90
$\Gamma_{15} \rightarrow \Gamma_{25}$	13.2	15.2	17.2	13.9	17.6	15.7	14.0	12.67	13.00
$L_3 \rightarrow L_2'$	9.5	10.2	-	8.9	12.7	11.3	10.3	9.86	9.42
$L_3' \rightarrow L_3'$	12.9	16.0	-	14.7	17.3	-	14.4	12.26	13.10
$X_5' \rightarrow X_1$	10.5	12.5	12.8	11.7	14.2	11.9	12.3	10.43	10.20
$X_5' \rightarrow X_3$	11.8	11.4	13.4	10.1	14.2	12.8	11.3	10.35	10.50

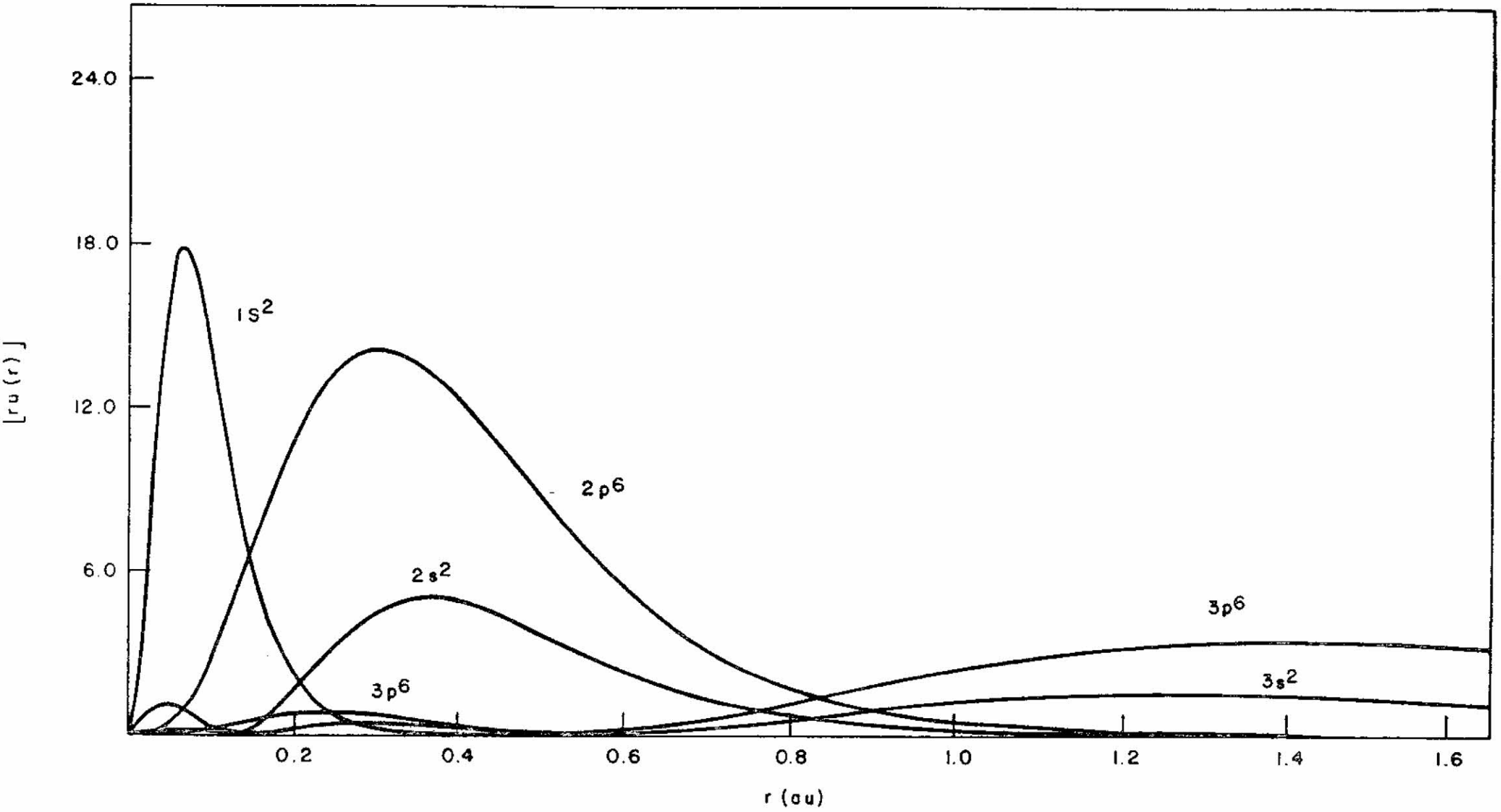

Fig. 1a. I. C. da Cunha Lima et al.

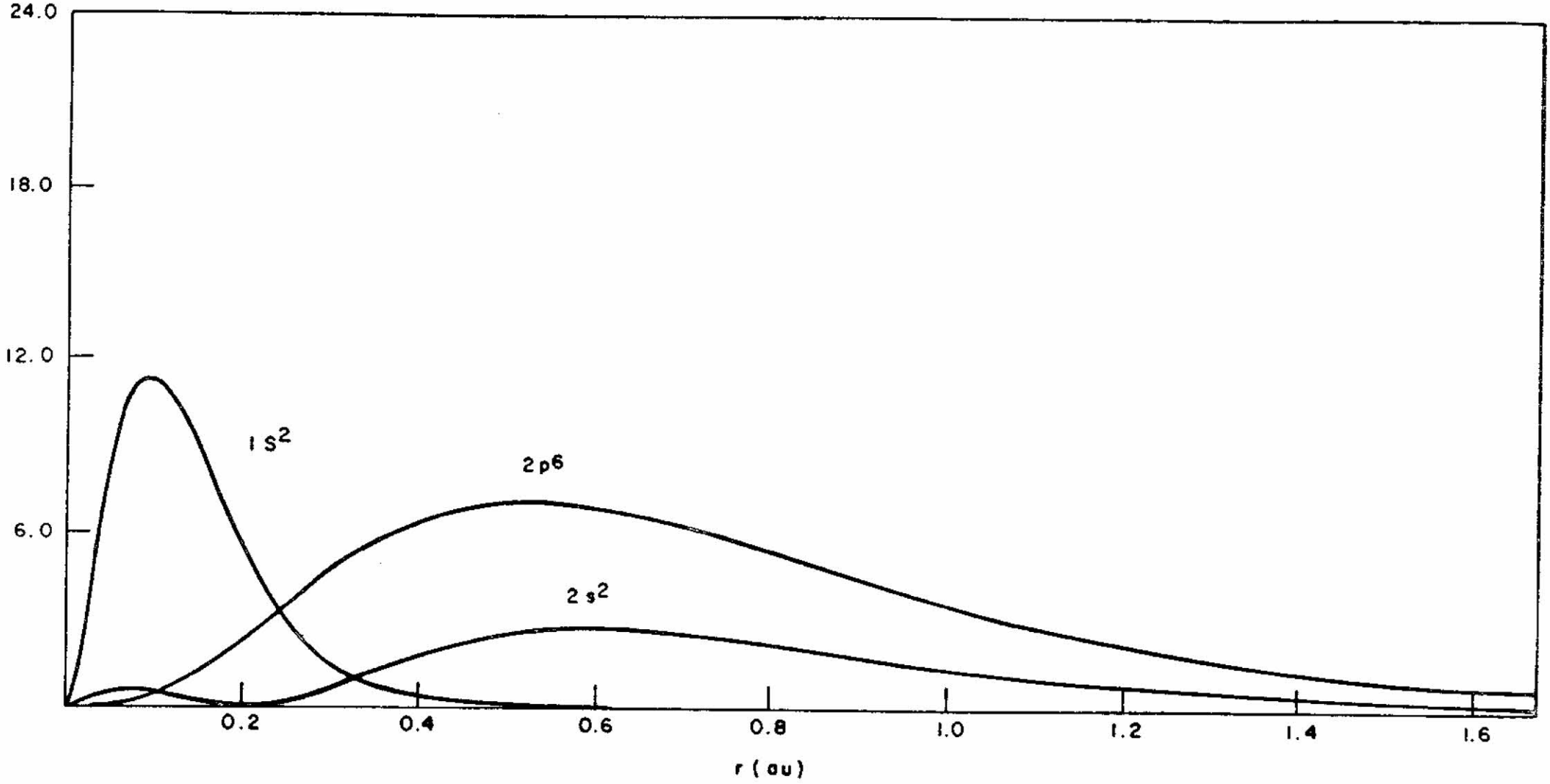

Fig. 1b - I. C. da Cunha Lima et al.

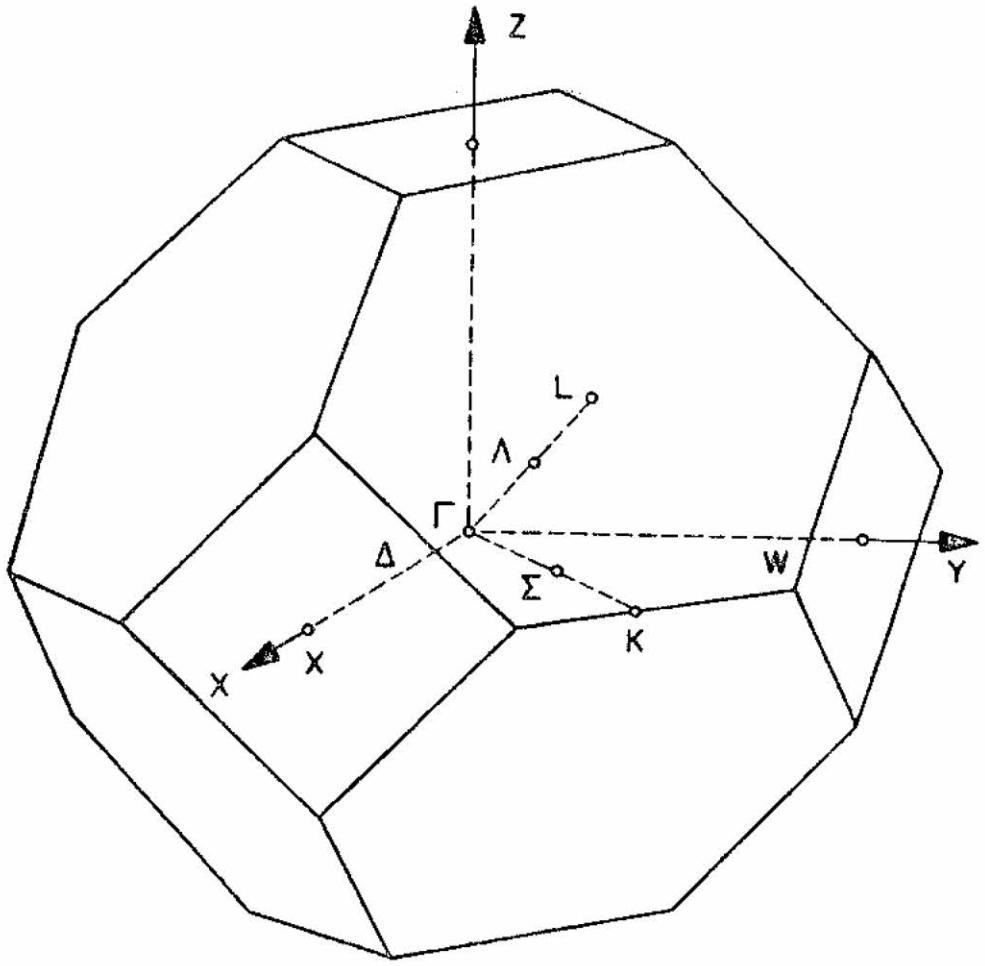

Fig. 2 I. C. da Cunha Lima et al.

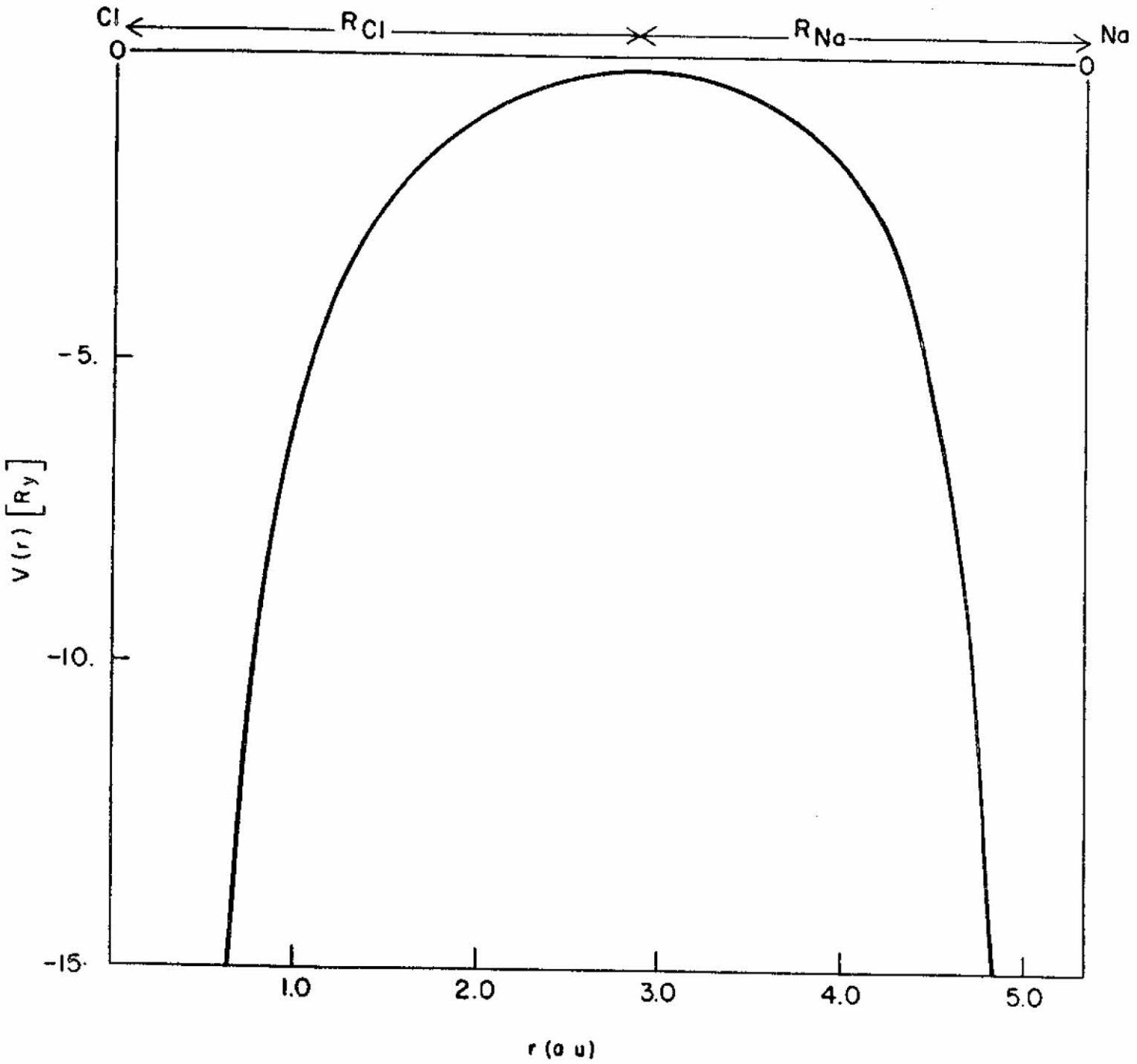

Fig. 3 - I. C. da Cunha Lima et al.

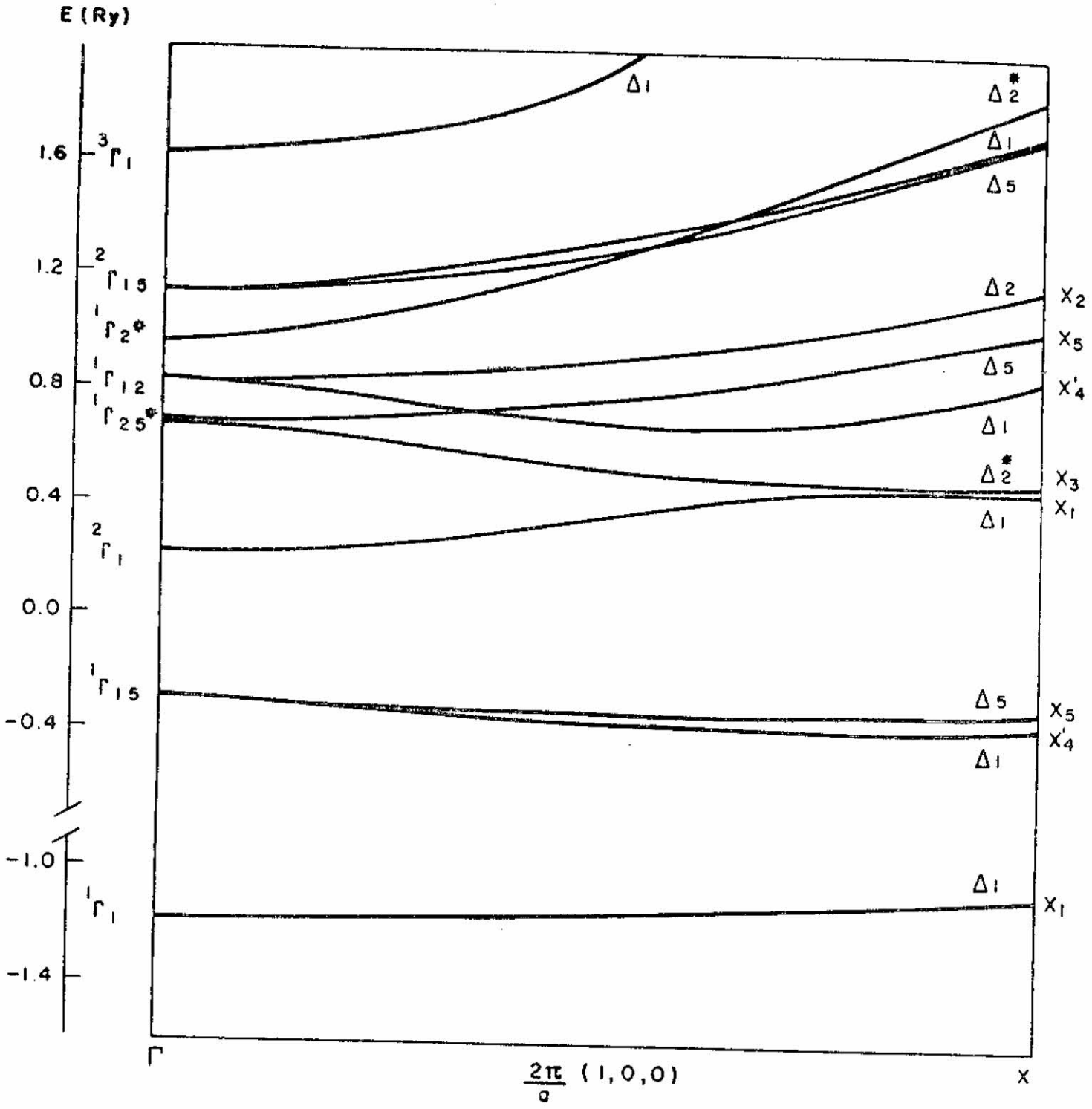

Fig. 4a. - I. C. da Cunha Lima et al.

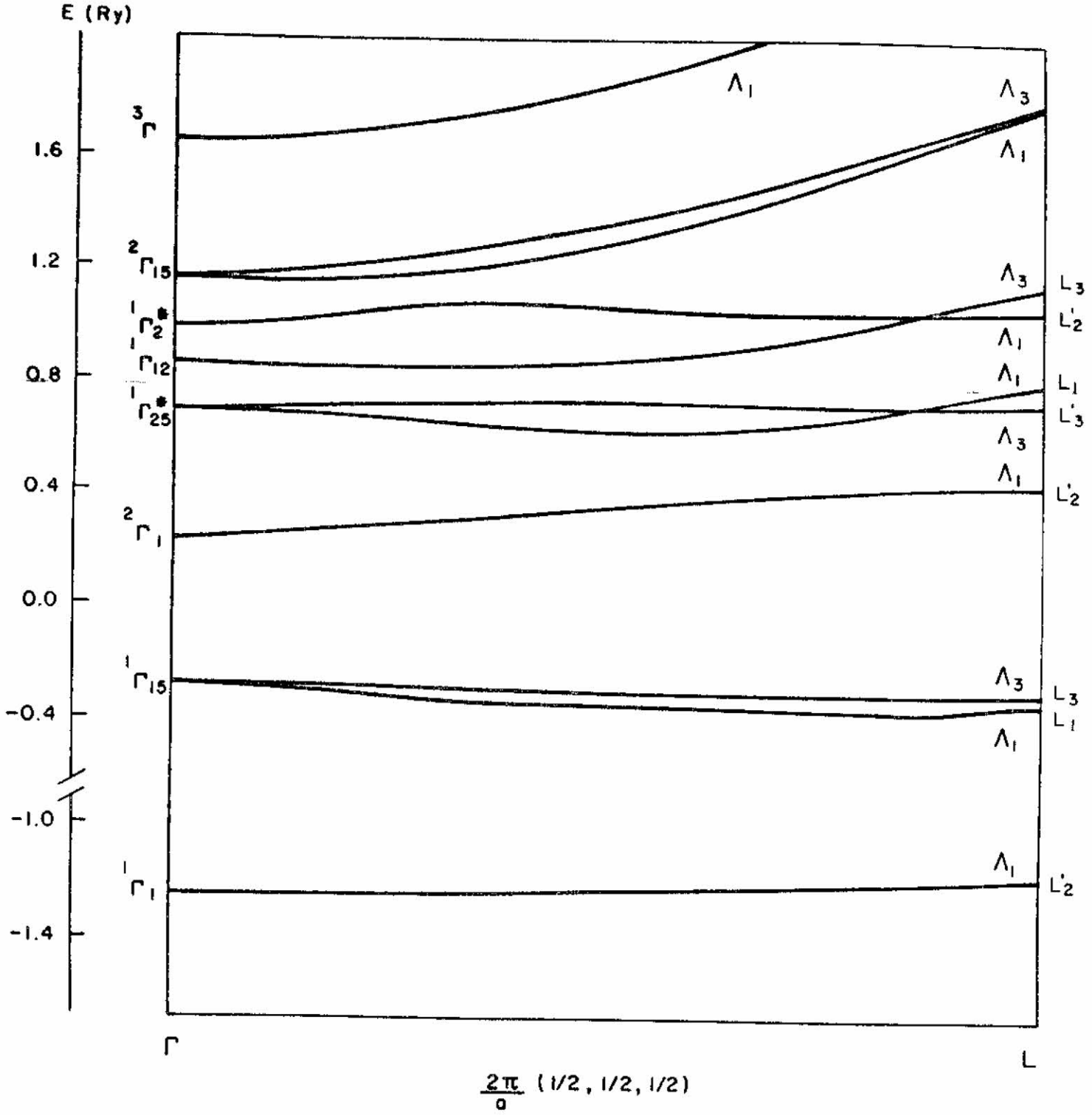

Fig. 4b - I. C. da Cunha Lima et al.

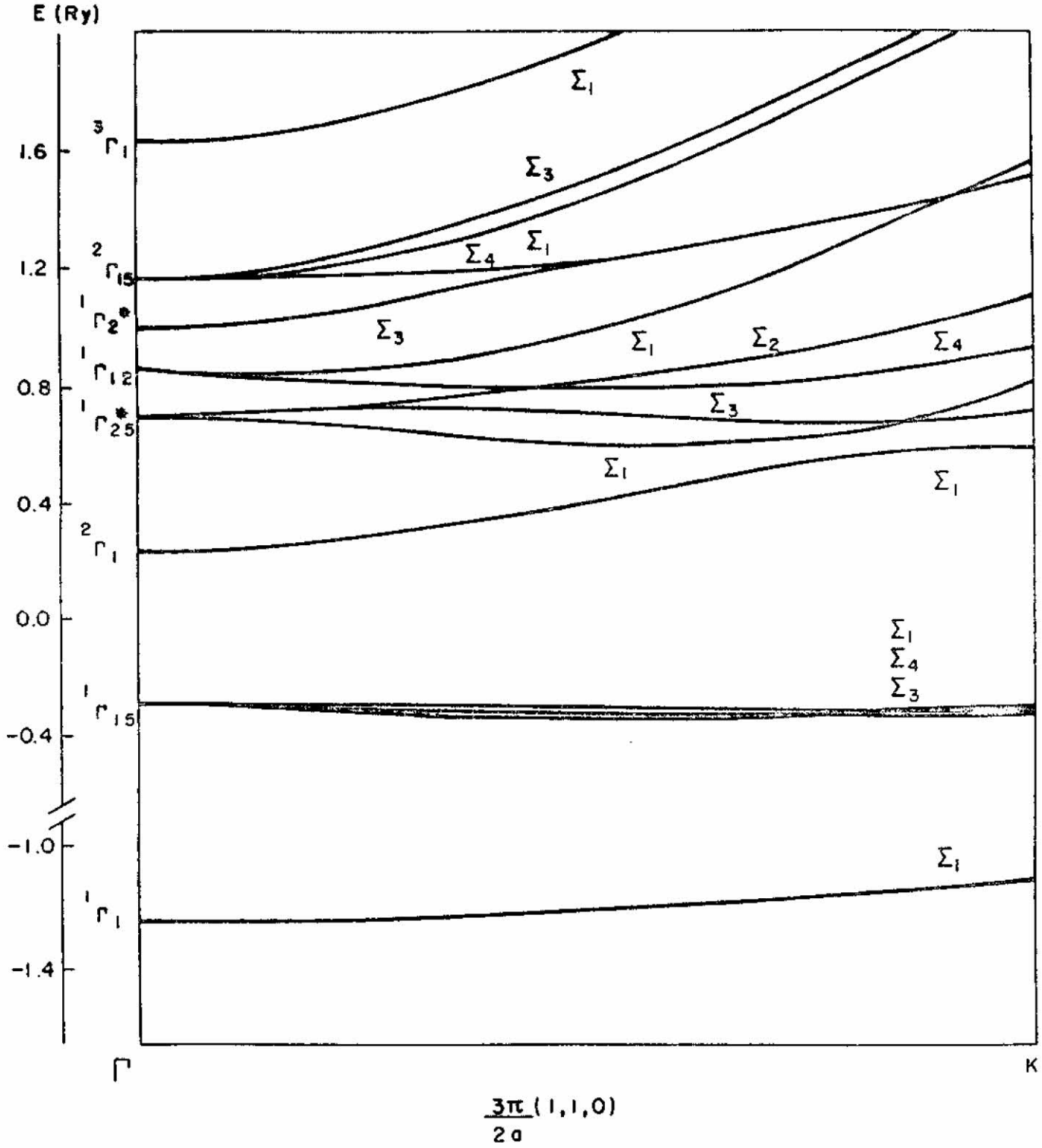

Fig. 4c - I. C. da Cunha Lima et al.